JOURNAL OF IMAGING SCIENCE AND TECHNOLOGY • Volume 42, Number 5, September/October 1998

Energy-level Assessment for Small Silver Clusters in AgBr Emulsion from Combined Experimental Data of Light Absorption, Spectral Sensitivity, and Photobleaching

Mitsuo Kawasaki* and Yoshiaki Oku

Department of Molecular Engineering, Kyoto University, Yoshida, Kyoto 606-8501, Japan

The combination of spectroscopic information concerning the light absorption, spectral sensitivity, and photobleaching involving the reduction sensitization centers allowed reasonable positioning of their electronic energy levels relative to the band edges of silver halides. A well-defined absorption band centered at 455 nm was observed both for the reduction sensitization centers produced by dimethylamine borane (DMAB) and for the hydrogen hypersensitization centers by using a diffuse transmittance spectroscopy method. We conclude that the common type of reduction sensitization centers, which must be predominantly hole trapping, have their HOMO (highest occupied molecular orbital) levels ~1.9 eV below the conduction band edge. Additional centers produced at the high level of DMAB sensitization have a higher HOMO level ~1.6 eV below the conduction band edge, which is identical with that previously ascribed to the subimage center. The dielectric polarization of the surrounding medium critically affects these energy levels. Possible limitations of the spectroscopic information as well as its advantages are also discussed.

Journal of Imaging Science and Technology 42: 409–415 (1998)

Introduction

Quantitative description of the process of latent image formation in photographic emulsion is a multidisciplinary work requiring a wide range of knowledge from elementary solid state physics to far more complicated heterogeneous chemistry. Nevertheless we still lack today convincing information in many respects even for the most fundamental electronic properties—the energy levels relative to the band edges of AgX—of the series of small Ag clusters on the emulsion grain surface pertinent to the imaging process. The difficulty stems in part from the inherently complicated emulsion format, but the major impediment seems to have been the extremely small size and small concentration at which such Ag clusters have been deemed to function in the photographic processes. Thus standard spectroscopy methods have seldom been considered useful to probe small Ag clusters in the photographic system, at least until the following breakthrough in the experimental characterization of the so-called reduction sensitization centers.

Judging from their negligibly small development-catalyzing capability the reduction sensitization centers must be certainly very small in size. However, it has been recently suggested that they could be present in regular reduction-sensitized emulsions in a concentration large enough to allow their absorption spectra to be measured by the conventional diffuse reflectance spectroscopy method.[1–3] Availability of such direct spectroscopic information certainly makes the cluster characterization easier and more reliable, together with all the other data made available by spectroscopy in one way or another.

The aim of this work is to show that combined experimental data of light absorption, spectral sensitivity, and photobleaching indeed lead us to infer a reasonable positioning of, in particular, the HOMO (highest occupied molecular orbital) level for the reduction sensitization centers, which are a prototype of small Ag clusters in photographic emulsion. We discuss major questions that have to be clarified to make proper energy level assessment for small Ag clusters in a dielectric medium, where in the dielectric relaxation effect plays a decisive role in the energetics of carrier trapping by Ag clusters. Through careful arguments, we can also illuminate both the limitations and advantages of spectroscopic information as the basis to establish the quantitative ordering of cluster energy levels for better understanding photographic processes.

Experimental

The AgBr emulsion consists of monodisperse octahedral AgBr grains with mean edge length of 0.45 μm, coated on a clear polymer support approximately 0.2 mm thick at a coverage of 1.0 g/m^2 in silver and 2.0 g/m^2 in gelatin. One of the two kinds of reduction sensitization centers studied here was produced in the normal mode of chemical sensitization with dimethylamine borane (DMAB) in the concentration range, 0.1~1.0 mg/mol-AgBr, for 40 min at 70°C. The other one is the hydrogen hypersensitization center produced in the otherwise unsensitized coating, by evacuating the sample with a turbo molecular pump for ~14 hr in advance and then storing it under 1-atm pure H_2 for 1 to 5 hr at ~50°C.

All the absorption spectra were obtained in the diffuse transmission mode by using the spectrometer illustrated in Fig. 1. Here a stack of typically 10 sample coatings (re-

---

Original manuscript received April 2, 1998

* IS&T Member; Corresponding Author

FAX: (+81)75-753-5526; E-mail: kawasaki@ap6.kuic.kyoto-u.ac.jp

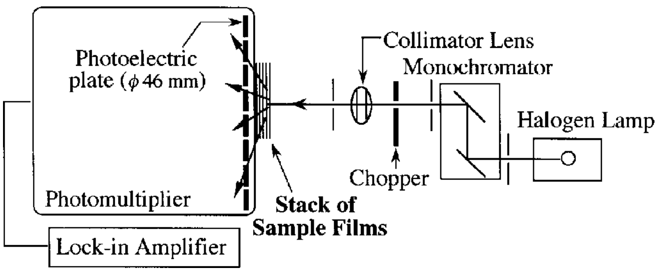

Figure 1. Experimental setup for diffuse transmittance measurement with a stack of emulsion coatings.

sulting in the total sample thickness of 2.5 mm including the film base) was mounted in close contact with an end-on photomultiplier tube, Hamamatsu Co., type R375, (Hamamatsu, Japan) with a large aperture size ~50 mm in diameter. This optical geometry ensures that the majority of the diffuse transmitted light is successfully captured by the photomultiplier. The principle of the measurement was described in a previous short article[4] and will be more fully discussed elsewhere in the future. Here it is sufficient to note that the product of the concentration and the absorption coefficient of the extra absorbing species incorporated in the emulsion coating should be proportional to the diffuse absorbance as defined by $\log T_0/T$. Here T and T_0 represent the diffuse transmittance values measured with and without the extra absorbing species, respectively.

The photobleaching experiment in the photoionization mode followed the method described in detail elsewhere,[5] but involved in this work samples in which a desensitizing dye, 1,1'-diethyl-2,2'-tricarbocyanine, was adsorbed as an effective electron acceptor to improve the bleaching efficiency. The merit of this dye is that its comparatively high oxidation potential [553 mV versus Ag/AgCl (Ref. 6)] minimizes hole injection from adsorbed dye that also could be excited by the bleaching exposure. This helps us to prevent the hole-induced bleaching from interfering with the photoionization-induced process.

The spectral sensitivity, or the long-wavelength sensitivity, was measured using the same apparatus as used for the photobleaching experiment. Thereby the long-wavelength sensitivity threshold was determined for sufficiently extended irradiation corresponding to the total photon flux of the order of $10^{17}/\text{cm}^2$.

Results and Discussion

Light Absorption Spectra. Figure 2 shows a typical diffuse absorbance spectrum taken for the DMAB-sensitized emulsion coating and its changes upon repeated scans with relatively heavy blue exposures in between scans. The clearly defined absorption signal due to the reduction sensitization centers was observed at a fixed position centered at 455 nm for all the DMAB-sensitized and hydrogen-hypersensitized samples when measured by our diffuse transmittance method, with the intensity proportional to the initial DMAB concentration or to the time of hydrogen treatment. This is substantially shorter than ~475 nm, which has been reported for similar reduction sensitization centers in other emulsions using the diffuse reflectance spectroscopy method.[1–3] Our observation is closer to the lowest energy transition involving simple diatomic Ag clusters in the gas phase[7] (~435 nm) or trapped in the low-temperature noble-gas matrices[7,8] (388 to 443 nm). Thus we attribute the 455 nm absorption to similar diatomic Ag clusters but adsorbed on the AgBr grain surface to serve as the reduction sensitization centers.

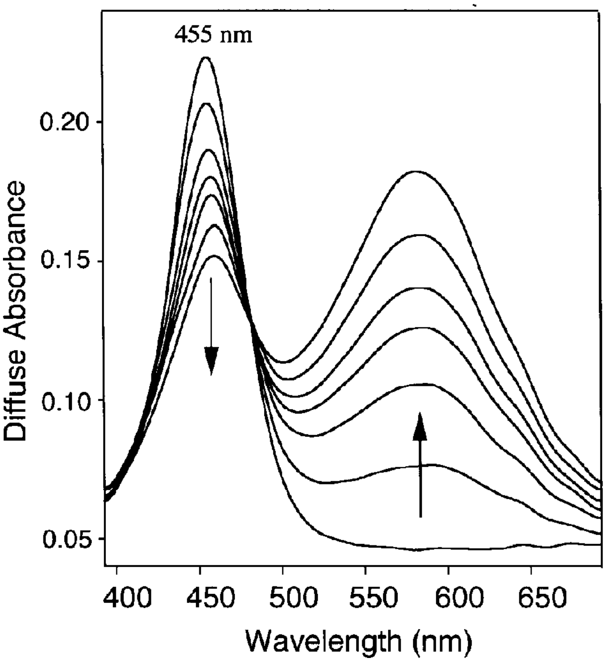

Figure 2. Typical diffuse absorbance spectrum of reduction sensitization centers produced by dimethylamine borane (DMAB; 1.0 mg/mol-Ag) and its changes upon repeated data acquisition with relative heavy blue exposure in between acquisitions.

More importantly, Fig. 2 indicates that the intensity decrease of the 455 nm absorption band in the course of the photolysis is accompanied by concurrent growth of a new broad absorption around 580 nm, with a clear isosbestic point at ~480 nm. This broad absorption represents the surface plasmon excitation of print-out silver particles, which are at least a few nm in size, and thus consist of hundreds or even thousands of Ag atoms. The appearance of the isosbestic point for the combination of the molecular cluster absorption and the plasmon absorption is really unique, suggesting that the print-out silver particles grow at the expense of the reduction sensitization centers in a fixed mass ratio.

The irreversible, sacrificial hole-removing function of the reduction sensitization centers provides the most straightforward explanation for this unique mass action effect, in such a way that the positive holes are eliminated irreversibly by the reduction sensitization centers and the resultant equivalent number of recombination-free electrons are subsequently utilized for the growth of the print-out silver. It has been argued that insofar as the reduction sensitization centers comprise Ag_2 species, they are not only capable of removing positive holes but may also generate an extra electron when they react with positive holes.[9] This attractive mechanism, if it really works, has only the effect of doubling the print-out yield. In any case the whole mechanism cannot be rationalized unless there is quite a large number of reduction sensitization centers on the individual AgBr grain surfaces. The large number density of reduction sensitization centers also follows from the relatively easy detection of the clear absorption signal by fairly simple spectroscopy methods.

Additional support for the hole-removing function of the reduction sensitization centers is presented in Fig. 3. Here the series of spectra were taken under the similar condition of blue exposure as in Fig. 2 but for samples dyed in advance with phenosafranine. To compensate for the strong overlapping absorption due to the phenosafranine dye, the

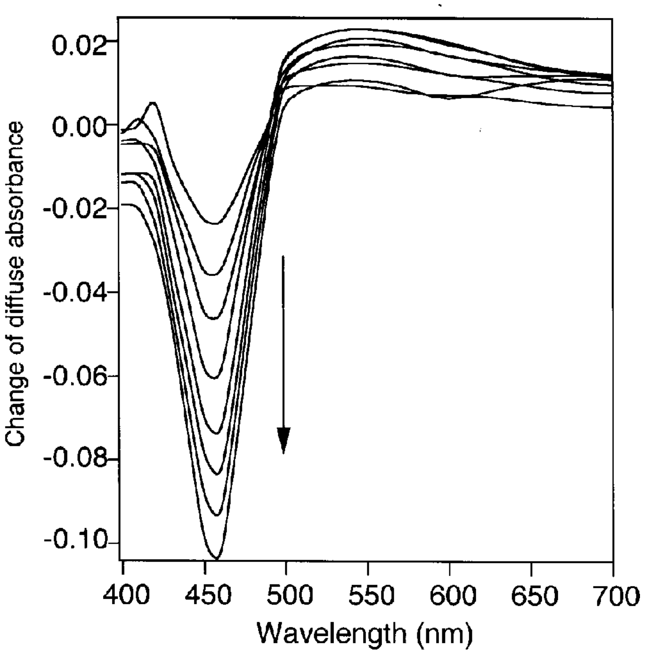

Figure 3. Series of diffuse absorbance spectra taken in similar condition of blue exposure as in Fig. 2, but for a DMAB-sensitized sample dyed with phenosafranine in advance. To compensate for the strong overlapping absorption due to the phenosafranine dye, the spectra are drawn in differential scale.

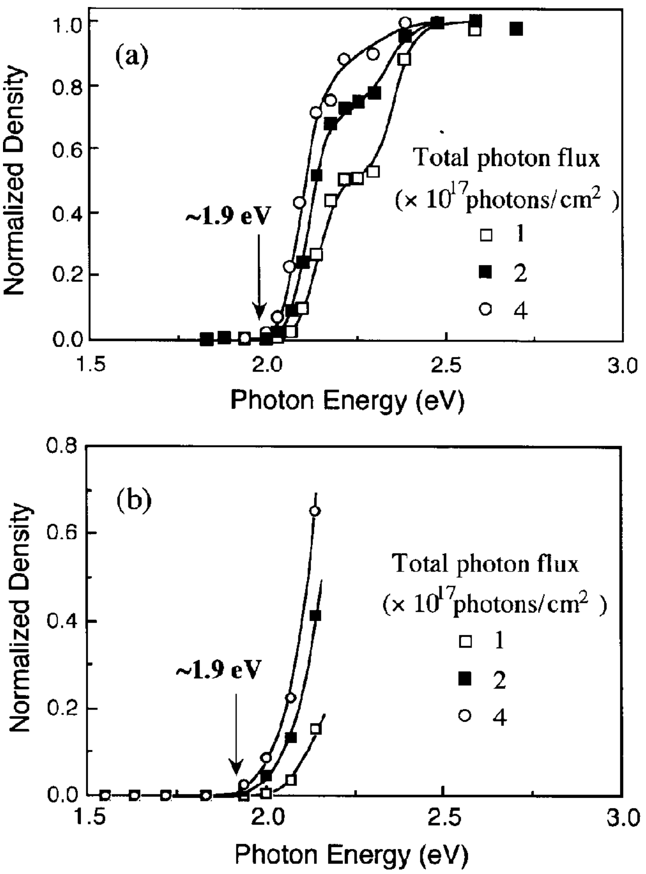

Figure 4. Long-wavelength sensitivity data obtained for samples given (a) low-level (0.1 mg/mol-Ag) DMAB sensitization and (b) hydrogen hypersensitization. Normalized density obtained by 10 min development in M-AA-1 after exposure to the total photon flux of the order of 10^{17}/cm^2 is plotted as a function of the photon energy.

spectra here are drawn in a differential scale. Phenosafranine is known as a typical desensitizing dye that strongly suppresses the formation of photolytic Ag clusters. As a result, the distinct plasmon absorption as seen in Fig. 2 is no longer visible in Fig. 3. Nevertheless, the 455 nm absorption due to the reduction sensitization centers is steadily bleached, because of irreversible reaction with positive holes.

Limiting Spectral Sensitivity and Photobleaching. We propose that the 455 nm absorption discussed in the preceding section represents the intramolecular HOMO→LUMO transition associated with the reduction sensitization centers. This is never the only allowed transition, however, insofar as these centers are adsorbed on the AgBr grain surface. Weak as it is, a charge-transfer type of electronic transition, or the photoionizing transition, may also occur from the HOMO level into the conduction band continuum of the host AgBr grain. The corresponding lowest excitation energy can be estimated from the long-wavelength sensitivity threshold or from the threshold of the photoionization-induced bleaching in the condition of total photon flux greatly exceeding that used for usual imaging purposes. Ironically it is this much weaker transition that carries the essential information about the HOMO level relative to the band edges.

Figure 4 shows typical long-wavelength sensitivity data obtained for the DMAB-sensitized sample corresponding to the lowest DMAB concentration [Fig. 4(a)] and for the hydrogen-hypersensitized (1-hr H_2 treatment) coating [Fig. 4(b)]. In both cases the sensitivity threshold for the sufficiently extended irradiation of the order of 10^{17} photon/cm^2 in total photon flux can be located at ~1.9 eV (~650 nm). This position was common to all the samples sensitized at relatively low DMAB concentrations (0.1 to 0.4 mg/mol-Ag) and to the hydrogen-hypersensitized coatings.

Note that the total photon flux of the order of 10^{17} photon/cm^2, used in the above experiment, is orders of magnitude greater than required to form latent image centers in the intrinsic region. For example, at 460 nm (2.7 eV photon energy) near the band edge, each grain can absorb just a few percent of the incident photons at most. In the case of our sample film, containing ~6.4×10^8 grain/cm^2, 10^{12} photon/cm^2 was sufficient to produce a developable image even in this tail region of intrinsic absorption. Thus the sensitivity threshold detected by using 10^{17} photon/cm^2 or more is due to an extremely weak transition corresponding to ~10^{-5}% absorption of the incident photons per grain, far below that detectable by, e.g., diffuse transmittance spectroscopy. In this context also worth noting is that we are now compiling additional evidence that suggests that the direct HOMO→LUMO transition at 455 nm causes noticeable spectral sensitization at the total photon flux of ~10^{12} photon/cm^2, which will be reported elsewhere in more detail. The total photon flux about 5 orders of magnitude greater than this, required to observe the ~1.9 eV threshold, in Fig. 4, is consistent with the proposed nature of the ~1.9 eV threshold, namely that the threshold stems from the much weaker photoionizing transition from the HOMO level of the reduction sensitization center to the conduction band continuum of AgBr.

As an alternative cause of the ~1.9 eV threshold, one might still think of something that could be associated with the AgBr grains themselves, made observable under the chemical sensitizing action of the reduction sensitization centers. Though such possibilities may not totally be

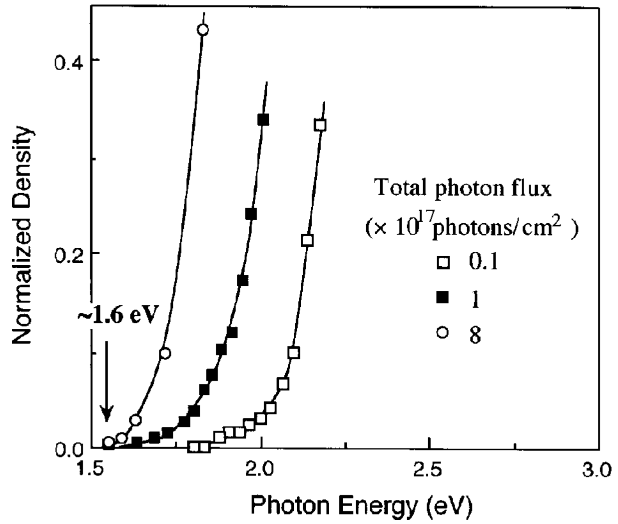

Figure 5. As in Fig. 4 but obtained for sample given high-level (1.0 mg/mol-Ag) DMAB sensitization.

ruled out at present, the fairly well-defined position of the threshold energy invariant over a wide range of sensitization conditions and total photon flux leads us to believe that the photoionizing transition involving the reduction sensitization centers is most relevant.

As shown in Fig. 5, at the highest level of DMAB sensitization the sensitivity threshold apparently moved further to the longer wavelength and reached ~1.6 eV. Such a discontinuous, sudden change in the threshold is also easier to understand in terms of the photoionizing transition by assuming that two different kinds of centers can be produced by the DMAB sensitization depending on sensitization level, even though we could observe only a single absorption band at 455 nm for the strongly allowed transition mentioned already. Note, however, that the centers responsible for the ~1.6 eV threshold do not necessarily represent the major product of the high-level DMAB sensitization. They more likely correspond to an additional center formed together with the common centers contributing to the ~1.9 eV threshold. Interestingly, the ~1.6 eV threshold almost exactly coincides with the photoionization threshold that we have previously ascribed to the two-atom subimage center formed in the imaging process.[5,10] This implies that the centers additionally produced by the high-level DMAB sensitization also could have an electron-tapping property similar to that of the subimage center. For simplicity we shall hereafter refer to the common reduction sensitization centers as R_I centers, while the additional ones that only appear at high-level DMAB sensitization as R_{II} centers.

The formation of R_{II} centers with potential electron-trapping capability by high levels of DMAB sensitization is further supported by the fogging characteristics shown in Fig. 6. While the samples sensitized at relatively low DMAB concentrations (thus possessing only R_I centers) exhibit only minor development fog even on extended processing for as long as 80 min in an M-AA-1 surface developer, the sample sensitized at the highest DMAB concentration (thus additionally carrying R_{II} centers) shows a steadily increasing fog with the development time, reaching almost the maximum developable density of our coating at the 80-min development time. This behavior is indeed similar to that expected for lightly pre-exposed AgBr grains with only subimage centers catalyzing the development.

Fortunately the large difference between R_I and R_{II} centers in their developabilities can be effectively used to detect R_{II} centers separately from R_I centers as extended-development-induced fog. As for the detection of R_I centers, we can utilize the gold-latensification method, based on the observation that all reduction-sensitized emulsions were invariably fogged more or less heavily when latensified with gold prior to the development. Of course, gold latensification may not discriminate between R_I and R_{II} centers so its application is limited to the samples carrying only R_I centers. In addition, it should be stressed that we never think that all of the R_I centers are converted to fog centers by gold latensification. If such a complete conversion occurred, one would not be able to discriminate even between grains with only one R_I center and those with a large number of R_I centers, both types of grains being invariably fogged by gold latensification. This situation would make the gold latensification a useless method for detection of R_I centers. In practice, only a minor fraction of R_I centers are converted to the fog centers in such a way that the developability, i.e., fog density, gained by gold latensification gives us information about the difference and/or changes in the number of R_I centers. This more desirable situation may also apply to extended development for detecting R_{II} centers.

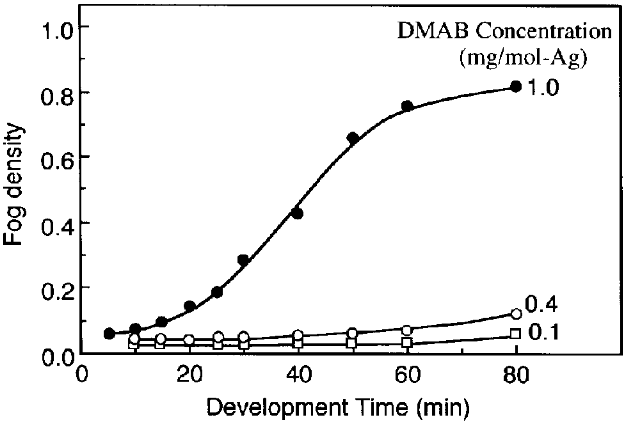

Figure 6. Fogging characteristics of a series of DMAB-sensitized coatings processed by M-AA-1 surface developer at 20°C. Numbers show the initial DMAB concentration in mg/mol-Ag used for the reduction sensitization.

The photobleaching experiment becomes feasible for both R_I and R_{II} centers now that their respective detection methods are established. Examples of the corresponding bleaching spectra are shown in Figs. 7(a) and 7(b). The decrease in the gold-latensification-induced-fog for the lowest level DMAB sensitization [Fig. 7(a)] or in the extended-development-induced fog for the highest level DMAB sensitization [Fig. 7(b)] is plotted as a function of the photon energy of the bleaching exposure. The bleaching thresholds found in these spectra, ~1.9 eV in Fig. 7(a) and ~1.6 eV in Fig. 7(b), agree well with the limiting spectral sensitivity thresholds for each sample as determined from Figs. 4 and 5. It was confirmed that the gold-latensification-induced fog for the hydrogen-hypersensitized coatings was also bleached with the same ~1.9 eV threshold as commonly assigned to R_I centers.

The close agreement between the limiting long-wavelength sensitivity threshold and the photobleaching threshold for both R_I and R_{II} centers strengthens our interpretation that both quantities represent the lowest transition energy from the HOMO levels associated with the reduction sensitization centers to the conduction band continuum of AgBr.

Energy Level Assessment. To correlate the present experimental data more specifically with the energy levels

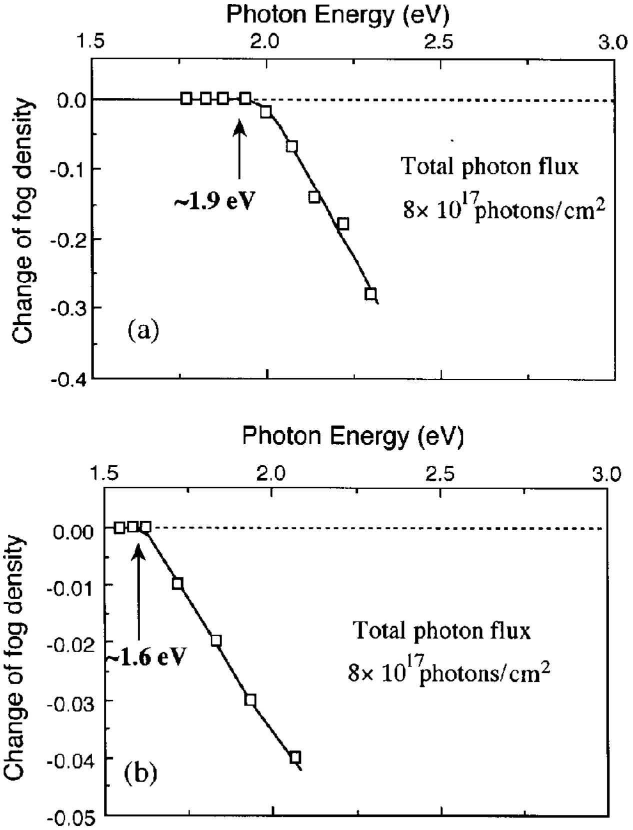

Figure 7. Photobleaching spectra of reduction sensitization centers detected as (a) gold-latensification-induced fog with low-level (0.1 mg/mol-Ag) DMAB sensitization and (b) extended-development-induced fog with high-level (1.0 mg/mol-Ag) DMAB sensitization.

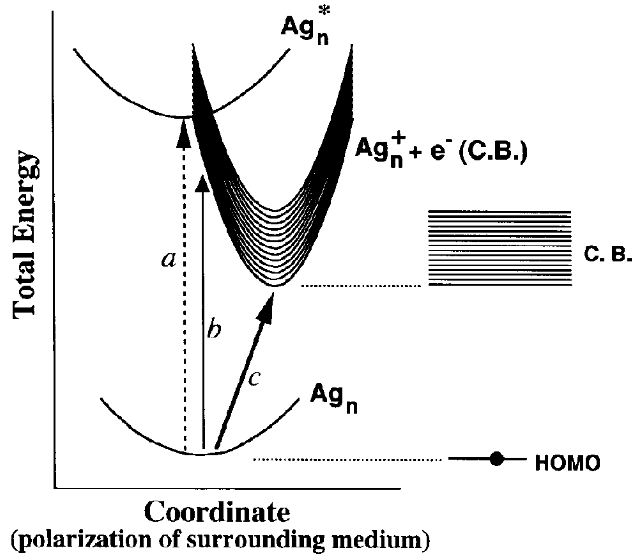

Figure 8. Potential energy diagram for a small silver cluster (bottom curve), lowest electronically excited state (top curve), and ionized state (middle curves) in dielectric medium. The coordinate represents dielectric polarization of surrounding medium. Arrows (*a*, *b*, and *c*) indicate intramolecular transition, vertical ionization, and adiabatic ionization, respectively. Simple energy-level diagram on the right side shows that ground-state HOMO level is defined by the adiabatic ionization energy. See text for more details.

of reduction sensitization centers, it is very helpful to refer to the adiabatic potential energy diagram as shown in Fig. 8. Here the lowest and the highest lying potential curves represent the total energies of a small Ag cluster (Ag_n: assumed to be electrically neutral) and its electronically excited state (Ag_n^*), respectively. The group of the middle-lying, closely spaced curves then represents the total energies of the ionized counterpart (Ag_n^+) plus an electron in the conduction band continuum. Note in addition that the coordinate we focus on here is the dielectric polarization of the AgBr substrate rather than the internal cluster coordinate. Thus the essential point being made in this diagram is that the total energy of a charged cluster (Ag_n^+ in this case) is much more sensitive to the dielectric polarization than that of an electrically neutral cluster. Accordingly the potential minimum for the ionized cluster is considerably shifted along the polarization coordinate with steep potential rise on both sides of the minimum. Now the HOMO level of the Ag_n relative to the conduction band edge is defined by the minimum energy required to remove an electron "adiabatically" from the Ag_n to the bottom of the conduction band, as illustrated in Fig. 8 by the conventional energy level diagram aligned side-by-side to the potential energy curves. Note that the difference between this adiabatic ionization energy and the vertical ionization energy becomes much greater in polarizable media than in the gas phase.

The spectral sensitivity threshold and the photobleaching threshold measured in this work represent the lower limit of photon energy capable of causing the photoionizing transition, which by no means corresponds to the energy at which the photoionization efficiency is maximized. Thus the threshold values, ~1.9 eV and ~1.6 eV assigned to R_I and R_{II} centers, respectively, may be understood to approach the adiabatic ionization energies or the HOMO energies relative to the bottom of the conduction band (see also the related discussion below.

It should be emphasized that the HOMO levels defined in this way are extremely sensitive to the difference in the dielectric stabilization between the initial (Ag_n) and final (Ag_n^+) states, as can be realized simply based on the potential energy curves shown in Fig. 8 at a qualitative level. For a more useful example, consider two kinds of spherical clusters, one neutral (Ag_n) and the other already carrying a partial positive charge, δe, in the initial state ($Ag_n^{\delta+}$), but otherwise identical with each other. Let us examine more quantitatively how the difference in the initial charge affects the HOMO level. To do so let I_n and I_c represent the adiabatic ionization energies required to remove the valence electron from Ag_n and $Ag_n^{\delta+}$, respectively. When both clusters are in vacuum one may simply write that

$$I_c(\text{vac}) = I_n(\text{vac}) + \frac{e^2\delta}{2R_1}, \qquad (1)$$

assuming that the valence electron ($-e$) in the positively charged cluster is under the extra Coulomb potential field around the δe charge at an effective radius of R_1, which may be approximated by the radius of $Ag_n^{\delta+}$ itself. The relation I_c (vac) > I_n (vac) as dictated by Eq. 1 means that in vacuum the HOMO level of the positively charged cluster becomes lower than that of the neutral one as naturally expected.

But in a polarizable medium with a relatively large static dielectric constant (ε), one has to take into account that there is a significant gain in energy (so-called solvation energy) by dielectric polarization whenever a charged center is taken from vacuum into the dielectric. In the case of the ionization of a neutral Ag_n, the positive charge (e) appears only in the final state. Thus the ionization energy corrected for the hydration energy in this final state is expressed by the following formula:

$$
\begin{aligned}
I_n(\varepsilon) &= I_n(\mathrm{vac}) - \frac{e^2}{2R_2}\left(1-\frac{1}{\varepsilon}\right) \\
&= I_n(\mathrm{vac}) - \frac{e^2}{2R_1}\left(1-\frac{1}{\varepsilon}\right) + f(R_1,R_2)
\end{aligned} \qquad (2)
$$

Here R_2 represents the effective radius of the ionized cluster, $\mathrm{Ag_n}^+$. The variable $f(R_1, R_2)$ in the modified expression of $I_n(\varepsilon)$ is a function depending on the difference between R_1 and R_2 and takes a negative value when δe is a partial positive charge (i.e., in the condition of $R_1 > R_2$). As for the ionization process involving $\mathrm{Ag_n}^{\delta+}$, the solvation energy comes into effect in both the initial state with δe charge and the more positive final state with $(1+\delta)e$ charge. The former tends to increase the net ionization energy while the latter causes the opposite effect, thus resulting in

$$
\begin{aligned}
I_c(\varepsilon) &= I_c(\mathrm{vac}) + \frac{(\delta e)^2}{2R_1}\left(1-\frac{1}{\varepsilon}\right) - \frac{[(1+\delta)e]^2}{2R_3}\left(1-\frac{1}{\varepsilon}\right) \\
&= I_c(\mathrm{vac}) - \frac{(2\delta+1)e^2}{2R_1}\left(1-\frac{1}{\varepsilon}\right) + g(R_1,R_3)
\end{aligned} \qquad (3)
$$

Here R_3 corresponds to the effective radius of $\mathrm{Ag_n}^{(1+\delta)+}$, satisfying $R_1>R_2>R_3$. The variable $g(R_1, R_3)$ in the second expression of $I_c(\varepsilon)$ is a function taking a more negative value than $f(R_1, R_2)$ in Eq. 2. From Eqs. 1 and 3 it follows that

$$
I_c(\varepsilon) = I_n(\mathrm{vac}) - \frac{e^2}{2R_1}\left(1-\frac{1}{\varepsilon}\right) - \frac{e^2\delta}{2R_1}\left(1-\frac{2}{\varepsilon}\right) + g(R_1,R_3). \qquad (4)
$$

When ε »1 all the $1/\varepsilon$ terms in the above equations can be neglected. Then by subtracting Eq. 4 from Eq. 2 we get

$$
I_n(\varepsilon) - I_c(\varepsilon) = \frac{e^2\delta}{2R_1} + f(R_1,R_2) - g(R_1,R_3) \; > 0, \qquad (5)
$$

because $g(R_1, R_3)$ takes a more negative value than $f(R_1, R_2)$ as mentioned already. Note that Eq. 5 also holds in the case where δe becomes greater than the unit charge, thereby $f(R_1, R_2)$ turns to a positive value. Equation 5 shows that, as opposed to the isolated clusters in vacuum, the HOMO level of the positively charged cluster goes above that of the neutral one in a dielectric medium. Though crude, such a simple electrostatic argument can give us a rationale for the conclusion that the HOMO level associated with $\mathrm{R_{II}}$ centers—likely having an electron-trapping property similar to that of the subimage center and thus potentially carrying a partial positive charge[11]—is located higher than that of $\mathrm{R_I}$ centers (~1.6 eV versus ~1.9 eV below the conduction band edge).

Note also that the above ordering of the HOMO levels for $\mathrm{R_I}$ and $\mathrm{R_{II}}$ centers does not contradict the relative reactivities with positive holes expected for these centers. As shown in our previous article[12] even latent image centers do react with positive holes. In other words, the reactivity of small Ag clusters with positive holes is determined kinetically, so as to be evaluated in terms of the capture cross section. This reactivity often scales inversely to the carrier-trapping depth, as was the case with the bleaching of latent image and subimage centers by positive holes.[12] Thus $\mathrm{R_{II}}$ centers, having a higher HOMO level to trap a positive hole deeper than in the case of $\mathrm{R_I}$ centers, may have a rather smaller capture cross section for positive holes. Moreover, the potential positive charge associated with $\mathrm{R_{II}}$ centers will reduce the rate of hole trapping further.

Once the HOMO level is fixed as discussed above, the direct HOMO→LUMO transition observed at 455 nm forces the corresponding LUMO level to be located well above the bottom of the conduction band (see the highest lying potential curve in Fig. 8). This intramolecular electronic transition does not alter the net charge of the cluster, so that the LUMO level estimated in this way may be approximately valid also in the adiabatic sense, if the intramolecular coordinate corresponding to the potential minimum is not much different between the ground and excited states. Note, however, that this LUMO level can be quite different from the level to which a photoelectron is actually trapped. The position of this real electron-trapping level must be defined by the energy released when an extra electron is added from the conduction band to the given center. The net charge of the cluster is thus altered between the initial and final states, and the polarization effect immediately comes up again.

An electrostatic model similar to that developed above may also be applicable to this complementary electronic process. We have to keep one important caution in mind however. For example, the addition of an extra electron to a neutral cluster produces a negatively charged cluster. Then one might think that, because of some large solvation energy for this negative charge in a dielectric medium, the net electron affinity therein could be significantly increased as compared to in vacuum. However, this is true only if the neutral cluster has a bonding orbital to accommodate the extra electron deep enough so that the resultant anion has a radius small enough to cause substantial dielectric polarization. In practice, relatively small neutral molecules, including the $\mathrm{Ag_2}$ molecule, seldom have an electron affinity greater than 2 eV with respect to the vacuum,[13] thus incapable of accepting an electron from the conduction band of AgBr, ~3.5 eV below the vacuum. Thus these molecules may not have a stable anionic state with a radius resulting in the gain of a meaningful level of solvation energy in a dielectric medium, and the dielectric argument is useless for such molecules. Thus it seems that very small silver clusters can take up an extra electron from the conduction band only when they carry a net positive charge. Even then the effect of dielectric polarization generally tends to reduce the electron affinity from that expected in vacuum, except for the case where the initial positive charge, δe, is smaller than $0.5e$. Only in this case does the charge in the final state, $(\delta - 1)e$, become larger in magnitude than the initial charge, δe, leading to the final state being stabilized more than the initial state. However, if electron trapping causes a large increase in the effective radius of the center at the same time, then the dielectric polarization may as well give the opposite effect (greater stabilization in the initial state) even in this particular condition of the initial positive charge.

In any case, for direct determination of the locations of such real electron-trapping levels, one needs somehow to measure either optical or thermal excitation spectra of the trapped electrons into the conduction band continuum. We stress again that it is only for comparatively large molecules such as organic dyes that the LUMO level can be used as an approximate measure for the electron-trapping level.

Limitations of Spectroscopic Data and Comparison with Nonoptical Methods. In our energy level assessment that focused upon the HOMO level of the reduction sensitization center, the threshold energies for limiting spectral sensitivity and for photobleaching are clearly of crucial importance. That these threshold energies are really associated with the photoionizing transitions involving the reduction sensitization centers may still be an assumption not necessarily fully justified as yet, but it allows the most straightforward interpretation of the whole of the experimental results. The validity of the proposed energy-level diagram may also be limited by the experimental accuracy in the threshold energies, but we trust that the maximum experimental error in our threshold determination should be no greater than ±0.1 eV, as also supported by the close agreement between the limiting spectral sensitivity threshold and the photobleaching threshold.

One may still question if the photoionization threshold can really be equated with the adiabatic ionization energy. It is true that this correlation is strictly valid only if the ground-state potential energy (cf., Fig. 8) is so weakly polarization dependent that the thermally allowed range of the polarization coordinate extends way over to the point corresponding to the potential minimum of the ionized counterpart. This condition may best be satisfied with an electrically neutral cluster, but in general the experimentally observed photoionization threshold may still be larger than the real adiabatic ionization energy. Note, however, that the energy levels of small Ag clusters pertinent to the imaging process are often those relevant to the dynamic electron- or hole-trapping processes. These levels are essentially identical with those involved (in the case of the HOMO level) in the photoionization events. The photoionization threshold thus provides an upper limit of the practical HOMO level that can participate in the electron transfer process, if not precisely equal to the adiabatic level.

In addition to the optical methods, electrochemical energy-level assessment has played a central role in the development of spectral sensitization theory and has been occasionally employed also in the context of the redox properties of small Ag clusters. The use of the electrochemical techniques requires a special caution, however, when applied to the photographic system. When small Ag clusters on the AgBr grain surface trap photoelectrons or positive holes, what immediately follows is the dielectric (essentially ionic) polarization as discussed above, with a time constant of typically ~10^{-12} s. In addition to this very rapid relaxation of the surrounding medium, either negatively or positively ionized Ag clusters after the carrier trapping are further subject to secondary ionic events involving the interstitial silver ions, which may substantially alter the cluster size. This is a much slower process than the dielectric polarization, but the corresponding time constant, 10^{-7} to 10^{-6} s at room temperature, is still very short compared to the time scale of conventional electrochemical measurements. Thus to electrochemically extract the information about the HOMO level of an arbitrary Ag cluster, as defined in Fig. 8, one virtually has to freeze the secondary ionic process and realize—at least approximately or temporarily on the time scale of the measurement—a simple reversible electron-transfer equilibrium between the given sized neutral cluster and its ionized counterpart. This is an extremely difficult condition to achieve experimentally. In principle, it seems that a redox equilibrium between two silver clusters having different sizes can be realized relatively easily by including a silver ion as the oxidized species, but this is never the simple electron-transfer equilibrium essential for the electrochemical energy-level assessment. Rather the simple electron-transfer equilibrium and the composite redox equilibrium involving a silver ion are often mixed up in the literature. The necessity of optical methods is best recognized in this circumstance, and the fundamental physics involved in the photoionization measurement, as suggested in Fig. 8, ensures that the method allows us to infer the most reasonable positioning of the HOMO levels relevant in the photophysics involving small Ag clusters.

Summary and Conclusion

Reduction sensitization centers in photographic emulsion are a prototype of small Ag clusters adsorbed on AgBr grains surface that play an important role in the photographic processes. Interestingly, they can be produced in a sufficiently large number density so that their light absorption signal can be detected easily using conventional spectroscopic methods. Our own method based on diffuse transmittance spectroscopy successfully uncovered a clearly defined absorption band centered at 455 nm both for reduction sensitization centers produced by dimethylamine borane and for hydrogen hypersensitization centers.

Combining of this direct spectroscopic information concerning light absorption with other spectroscopic data concerning limiting long-wavelength sensitivity and photoionization-induced bleaching, all of which were taken with the same series of model AgBr emulsion coatings, allowed reasonable positioning of the electronic energy levels, in particular the HOMO levels associated with reduction sensitization centers.

It has been concluded that the common type of reduction sensitization centers produced as the major product of reduction sensitization or hydrogen hypersensitization have their HOMO levels ~1.9 eV below the silver bromide conduction band edge. Additional centers formed at the high level of DMAB sensitization exhibit properties analogous to those of subimage centers and have higher HOMO levels ~1.6 eV below the conduction band edge. The position of these levels is critically affected by the dielectric polarization of the surrounding medium.

The LUMO levels of the reduction sensitization centers are located well above the bottom of the conduction band, based on the position of the HOMO level and our assignment of the direct HOMO→LUMO transition observed at 455 nm. However, this level can be quite different from the real electron-trapping level and is thus of little photographic significance.

Optical or spectroscopic information is vital for proper positioning of the electronic energy levels associated with the small Ag clusters in photographic emulsion. Whenever these clusters trap electrons or positive holes, the resultant ionized counterparts are immediately subject to secondary process involving interstitial silver ions, thereby the cluster size may be substantially altered. Unless the time scale of the measurement is shorter than this ionic process, one cannot have the required experimental access to the levels involved in the dynamic carrier trapping by Ag clusters.

Acknowledgment. We would like to thank Dr. Judith M. Harbison (retired) and Dr. Marian Henry of the Eastman Kodak Company for preparation of the series of DMAB-sensitized coatings used in this work.

References

1. T. Tani and M. Murofushi, *J. Imaging Sci. Technol.* **38,** 1 (1994).
2. S. Guo and R.K. Hailstone, *J. Imaging Sci. Technol.* **40,** 210 (1996).
3. A. G. DiFrancesco, M. Tyne, C. Pryor, and R. K. Hailstone, *J. Imaging Sci. Technol.* **40,** 576 (1996).
4. Y. Oku and M. Kawasaki, *J. Imaging Sci. Technol.* **42,** 346 (1998).
5. M. Kawasaki, T. Yoshiki, and Y. Oku, *J. Imaging Sci. Technol.* **37,** 568 (1993).
6. J. Lenhard, *J. Imaging Sci.* **30,** 27 (1986).
7. G. A. Ozin, *Faraday Symp. Chem. Soc.* **14,** 7 (1980).
8. S. Fedrigo, W. Harbich, and J. Buttet, *Phys. Rev. B.* **47,** 10706 (1993).
9. See, e.g., R. K. Hailstone, N. B. Liebert, M. Levy, and J. F. Hamilton, *J. Imaging Sci.* **35,** 219 (1991); T. Tani, *J. Imaging Sci.* **30,** 41 (1986).
10. M. Kawasaki, Y. Tsujimura, and H. Hada, *Phys. Rev. Lett.* **57,** 2796 (1986).
11. T. Tani, *Photogr. Sci. Eng.* **15,** 181 (1971); J. F. Hamilton and R. C. Baetzold, *Photogr. Sci. Eng.* **25,** 189 (1981).
12. Y. Oku and M. Kawasaki, *J. Imaging Sci. Technol.* **40,** 582 (1996).
13. D. R. Lide Ed., *CRC Handbook of Chemistry and Physics*, 75th ed., CRC Press, Boca Raton, FL, 1994, pp. 10–180.